5-10 GHZ ALN CONTOUR-MODE NANOELECTROMECHANICAL RESONATORS

M. Rinaldi, C. Zuniga and G. Piazza
Department of Electrical and Systems Engineering, University of Pennsylvania, Philadelphia, USA

ABSTRACT

This paper reports on the design and experimental verification of Super High Frequency (SHF) laterally vibrating NanoElctroMechanical (NEMS) resonators. For the first time, AlN piezoelectric nanoresonators with multiple frequencies of operation ranging between 5 and 10 GHz have been fabricated on the same chip and attained the highest *f-Q* product (~ 4.6· 10^{12} Hz) ever reported in AlN contour-mode devices. These piezoelectric NEMS resonators are the first of their class to demonstrate on-chip sensing and actuation of nanostructures without the need of cumbersome or power consuming excitation and readout systems. Effective piezoelectric activity has been demonstrated in thin AlN films having vertical and lateral features in the range of 250 nm.

I. INTRODUCTION

In recent years the use of Nanoelectromechanical systems (NEMS) for a large number of applications spanning from semiconductor based technology to fundamental science [1] has been extensively explored. In particular, NEMS resonators have been exploited as transducers suitable for the realization of extremely sensitive gravimetric sensors. Sub-attogram mass resolution has been demonstrated in NEMS cantilevers [2] thanks to the minuscule mass and the relatively high quality factor (*Q*).

A fundamental figure of merit for all resonant sensors is the *f-Q* product. In fact, the mass sensitivity of the resonator scales with the square of its frequency of operation while the minimum detectable frequency shift is intrinsically related to the frequency stability of the device, hence to the inverse of its quality factor [3]. High *Q* values have been measured for nanoresonators [4], but frequencies of operation have been limited to the UHF range. In order to take full advantage of scaling laws of miniaturization and achieve higher values of sensitivity and figure of merit than corresponding macroscale counterparts (*i.e.* quartz crystal-based sensors), NEMS resonators should operate in the SHF band (3 – 30 GHz).

The greatly reduced dimensions of the NEMS devices demonstrated to date make them very sensitive to added mass, but also render their transduction very hard to implement [5]. In particular, the most common sensing and actuation techniques (piezoelectric and electrostatic) employed for MEMS devices have not been directly applied to the NEMS domain, due to the increase of parasitic effects associated with both the scaled dimensions of the devices and their higher frequency of operation.

In this paper, fundamental transduction problems in NEMS resonators are solved by using on chip piezoelectric actuation and sensing of Aluminum Nitride (AlN) nanostructures. In addition, previously unexplored frequencies of operation for NEMS resonators in the 5-10 GHz range are demonstrated on the same chip and high quality factors between 400 and 700 are attained in ambient conditions. This work experimentally demonstrates the highest *f-Q* product ever achieved in NEMS resonators (~ 4.6· 10^{12} Hz).

These results have been made possible by exploiting the excellent scaling capability of the AlN contur-mode technology. Resonance frequencies in the SHF band have been obtained by piezoelectric excitation of nano-strips (500-1000 nm wide) of AlN in their contour–extensional mode of vibration (contrary to flexural vibrations generally employed in the NEMS devices demonstrated to date). At the same time, the increase of parasitic effects associated with the reduced dimensions of these AlN nano-strips has been overcome by mechanically coupling a large number (49-99) of these devices (Fig. 1). In this way all the nanoresonators comprised in the resulting array can be directly actuated and sensed piezoelectrically and are mechanically forced to simultaneously vibrate at the same frequency. Finally, a high *Q* factor in air has been demonstrated by taking advantage of the intrinsic high quality of the AlN nano-film (250 nm thick) grown directly on top of a silicon substrate.

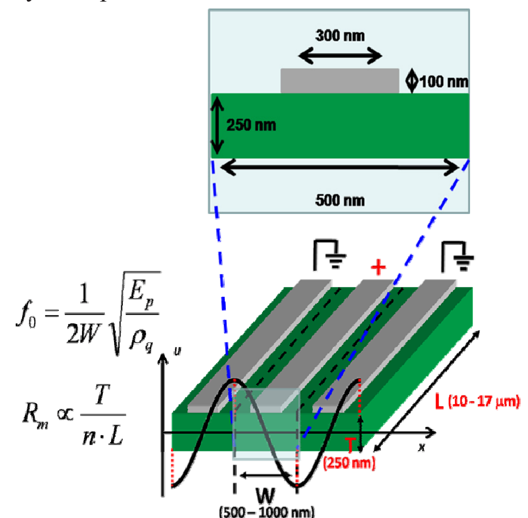

***Figure 1**: Schematic representation of three mechanically coupled AlN nanoresonators: the resonance frequency of the overall system is set by the width (W) of the single nanoresonator. The frequency determining dimension is effectively uncoupled from the overall dimensions of the AlN nano-plate; therefore, the number (n) of nano-strips and their length (L) can be arbitrarily adjusted to set the motional impedance (R_m) of the resonator.*

A similar range of frequencies and quality factors have been demonstrated in thickness-extensional film bulk acoustic resonators (FBARs) [6]. Differently from, FBARs, laterally vibrating contour-mode NEMS resonators can easily offer multiple frequencies of operation on the same silicon chip, and, from a fundamental physics perspective, have shown, for the first

time, piezoelectric excitation of nanoscale lateral features. The ability to define multi-frequency devices on the same die constitutes a breakthrough in the demonstration of multi-band communication devices and sensing platforms with extended sensitivity range.

II. NEMS RESONATOR DESIGN

High performance AlN contur-mode MEMS resonators in the frequency range of 20-1700 MHz and quality factor between 1000 and 3000 have been previously demonstrated [7,8]. Piezoelectric sensing and actuation of these devices have been successfully employed in the MEMS domain. Resonators with motional impedance as low as 50 Ω have been demonstrated, therefore making the interface of these devices with RF electronics relatively easy to implement.

According to the working principle of AlN contour-mode resonators, the application of an electric field across the thickness of the AlN film causes an in plane deformation of the structure through the equivalent d_{31} piezoelectric coefficient and excites the resonator in a contour-extensional mode of vibration. The resonance frequency of these devices can be lithographically set as expressed in equation (1)

$$f_0 = \frac{1}{2W}\sqrt{\frac{E_0}{\rho_0}} \qquad (1)$$

where W is the width of the resonator and E_0 and ρ_0 are respectively the equivalent Young's modulus and density of the AlN. In this way, in a rectangular plate, one device dimension (W) sets the resonance frequency whereas the other two (length, L, and thickness, T) can be used to define the equivalent motional impedance of the resonator [8]:

$$R_m \propto \frac{T}{L} \qquad (2)$$

From a scaling perspective, this is an important advantage of the AlN contour-mode technology over electrostatically-transduced resonators for which frequency scaling is generally associated with an increase in device impedance [9]. Even if improved device impedance with higher frequency of operation has been demonstrated using internal dielectric transduction [10], the achieved value of impedance is still considerably high.

In this work, the device dimensions are scaled to the nano realm both in the lateral (W) and vertical (T) direction (Fig. 1) in order to increase the frequency of operation while keeping relatively small values of motional resistance. The sub-micron width of the AlN nano-strip (Fig. 1) sets the resonance frequency in the SHF band, while an extremely thin AlN film (250 nm) increases the intrinsic electrical capacitance associated with the device to values above the substrate parasitics. Considering the reduced thickness of the AlN nano-strip, its length (L) is proportionally scaled in order to maintain a T/L ratio close to the one employed in MEMS devices. Even if a longer device would effectively yield a smaller motional resistance (eq. 2), the increase in length is associated with a higher electrical resistance in the electrodes, which directly affects the device Q factor. Therefore, the length of the device is set taking into account the trade-off between decrease in motional resistance and increase in electrical resistance associated with the metal electrode.

In order to further reduce the motional resistance of the resonator and increase its electrical capacitance, which are both essential conditions to enable the device on chip actuation and sensing, a large number of AlN nano-strips are mechanically coupled into an array. According to this strategy, the final NEMS device is formed by an array (varying from 49-99) of mechanically coupled nano-strips of AlN (width of 500-1000 nm). The overall motional resistance proportionally decreases by the number (n) of mechanically coupled nano-strips, while the electrical capacitance increases by the same factor.

Differently from any previously demonstrated AlN contour-mode device, the very thin film of AlN (250 nm) is directly grown on top of a Si substrate. No bottom electrode is employed in order to maintain extremely high quality AlN in each of the nano-strips (rocking curve value of 2.1° was obtained and it is comparable to micron-thick films). Consequently, a scheme based on lateral field excitation (LFE), which requires solely a top electrode, is adopted to set contour-extensional vibrations in each of the nanostrips. An alternating electric field is applied across the thickness of each AlN nano-strip by coplanar signal and ground electrodes patterned on top of the AlN nano-plate (Fig. 2). Since all the AlN nano-strips are mechanically coupled, a lamb-wave like mode is excited in the nano-plate (Fig. 2).

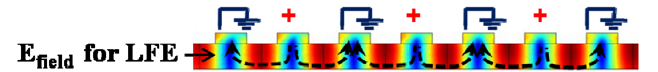

***Figure 2**: Results of FEM analysis of the mode of vibration of a 8.5 GHz resonator composed of 89 mechanically coupled nano-strips of AlN. The figure shows only few of the sub-resonators as representatives of the overall device behavior.*

III. FABRICATION PROCESS

The AlN NEMS resonators are fabricated combining optical and electron-beam lithography techniques. A simple 3 mask, potentially post-CMOS compatible (T_{max}< 400 °C), fabrication process has been employed (Fig. 3). The thin AlN film (250 nm) is directly grown on top of a high resistivity Silicon wafer. Optical lithography is first performed for the definition of both the device contact pads and the alignment markers for the subsequent electron-beam lithography step. Then, the in-plane dimensions of the AlN nano-plate are defined by ICP etching in a Cl_2-based chemistry using photoresit as a mask. Afterwards, electron-beam lithography is performed to define the sub-micron electrodes necessary to excite each nano-strip of AlN. Finally, the resonator is released from the Si substrate by isotropic dry etching in XeF_2.

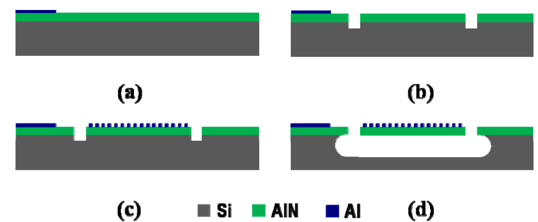

***Figure 3**: Basic steps for fabrication of the AlN NEMS resonators. (a) Optical lithography and lift-off of Al (100*

nm thick). (b) Dry etching of the AlN in Cl_2 . (c) Electron-beam lithography and lift-off of the sub-micron Al electrodes (100 nm thick). (d) Nanoresonator release in XeF_2.

It is important to note that, although electron-beam lithography was employed, the minimum feature size (300 nm) can also be defined by state-of-the-art optical lithography conventionally used in CMOS foundries, therefore making this device amenable to large scale manufacturing.

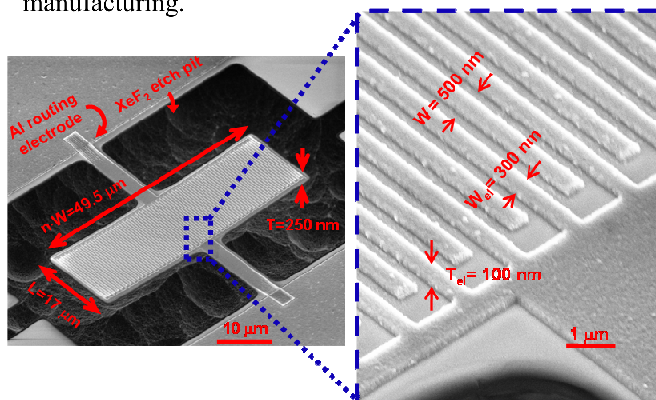

***Figure 4**: SEM picture of a fabricated 9.9 GHz NEMS resonator with zoomed view of the nano-strip array (nano-strip width is 500 nm; electrode width is 300 nm).*

An SEM picture of one of the fabricated devices is shown in Figure 4. In this case, the overall dimensions of the mechanically coupled AlN nano-strip array ($n = 99$) are approximately 17 x 49.5 µm.

IV. RESULTS AND DISCUSSIONS

The fabricated AlN NEMS resonators were tested in an RF probe station and the admittance curves of the devices were measured by an Agilent® N5230A Network Analyzer after performing a short-open-load (SOL) calibration on a reference substrate. Furthermore, in order to access the true electrical response of the device a de-embedding procedure to eliminate pad parasitics was performed [11]. The value of parasitic capacitance associated with the substrate was found to be approximately 16 fF.

The admittance curve of an 8.5 GHz resonator after de-embedding is shown in Figures 5 and 6. As in all other tested devices a single sharp resonance is attained at the designed mode of vibration between 2.5 and12 GHz.

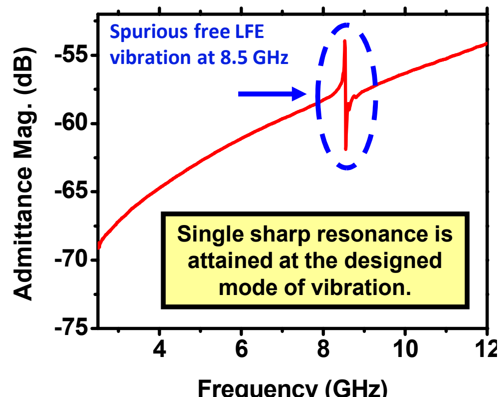

***Figure 5**: Electrical response of a fabricated 8.5 GHz nanoresonator.*

The measured responses of the fabricated devices were fitted to the Butterworth van Dyke (BVD) model and the equivalent electrical parameters were extracted (Fig. 6). Moreover, 2D Finite Element Method (FEM) analysis using COMSOL Multiphysics was performed in order to evaluate the experimental performances of these nanoresonators and verify that all the properties of AlN film were preserved when scaled to the nano realm. In the FEM analysis, the quality factors of the devices were forced to match the experimental values, since they cannot be predicted a priori trough FEM simulation.

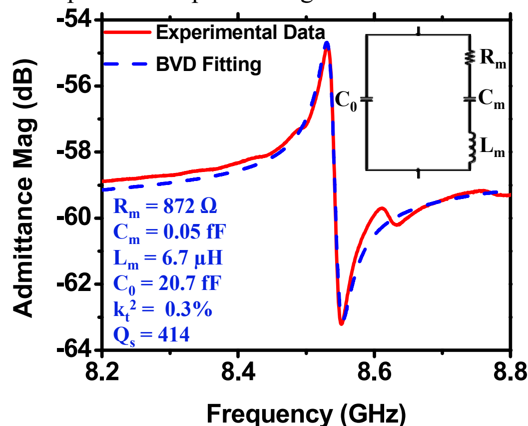

***Figure 6**: Butterworth van Dyke (BVD) model fitting and parameters extraction for a fabricated 8.5 GHz nanoresoantor.*

The electromechanical parameters extracted by BVD fitting both FEM analysis and experimental response of a 8.5 GHz resonator are compared in Table 1. Considering the very good agreement between FEM analysis and actual experimental response it is possible to conclude that the AlN physical and piezoelectric properties are conserved in the fabricated nanoresonators.

***Table 1**: Electromechanical parameters extracted from FEM analysis and experimental response of a 8.5 GHz nanoresonator.*

Extracted Parameters	**FEM Simulations**	**Experimental Data**
f_0	8.544 GHz	8.526 GHz
C_0	23 fF	20.7 fF
R_m	900 Ω	872 Ω
k_t^2	0.31%	0.3%

Comsol simulations also closely predict the frequencies of vibration of the AlN NEMS resonators. A discrepancy of less than 0.25% was found between FEM analysis and experimental data, further proving that the actual behavior of this new class of nanodevices can be described by conventional models valid for larger structures.

The measured resonance frequencies and the respective values of quality factor (Q_s) in air for all the fabricated nano devices are reported in Table 2. The best $f{\cdot}Q$ value that was achieved ($4.58{\cdot}10^{12}$ Hz) is approximately 2.5 times higher than what has ever been reported for AlN contour-mode MEMS resonators [8,12] and it is the highest ever measured for nanoelectromechanical devices.

The same electrical measurements were also

performed in vacuum and showed a slight improvement in *Q* (approximately 10%). Although the improvement is not significant, it is still a sign that surface effects need to be taken into account in the design of these NEMS resonators.

Table 2*: Dimensions and measured performances of the fabricated devices.*

Width (W) and number (n) of AlN nano-strips	f [GHz]	Q_s	$f\cdot Q_s$[Hz]
W=1000 nm, n=49	5.2	740	$3.85\cdot10^{12}$
W=700 nm, n=69	7.3	627	$4.58\cdot10^{12}$
W=600 nm, n=89	8.5	414	$3.52\cdot10^{12}$
W=500 nm, n=99	9.9	202	$4.16\cdot10^{12}$

The temperature coefficient of frequency (TCF) of the fabricated nano resonators was also measured and found to be - 35.8 ppm/°C. This value is higher than what is encountered in equivalent MEMS devices [13]. This is due to the effect of the Al electrodes, whose thickness (100 nm) becomes a considerable fraction of the AlN (250 nm) film in the NEMS implementation. Indeed, accounting for the temperature coefficient of Young's modulus of Al (about 10 X that of AlN), the analytical model fits the experimental data (Figure 7). The TCF of these NEMS resonators can be reduced by decreasing the thickness of the metal electrodes or by employing metals with temperature coefficient of Young's modulus lower than the one of Al (*i.e.* Pt). In addition, total temperature compensation can be achieved by depositing on the top surface of the NEMS resonators a material with positive TCF (such as SiO_2) in the same way it has been previously demonstrated for MEMS AlN resonators [13].

Finally, the sensitivity to mass per unit area of the fabricated devices was estimated accordingly to [14]. Device sensitivity as high as 6 MHz·μm^2/fg at 9.9 GHz was extracted. This value is approximately 10 X higher than what has been recently reported for nano cantilever devices [2]. This shows the great potential of the nanoresonators presented in this paper for gas sensing applications. The combination of high frequency of operation, high quality factor in air, large surface area available for sensing and on-chip transduction make these NEMS AlN technology the best candidate for the development of volatile organic chemical sensors.

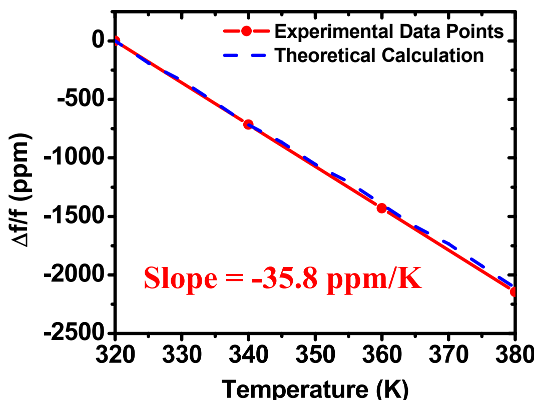

Figure *7: Experimental measurement of the TCF of the fabricated 8.5 GHz NEMS resonator compared with its analytical prediction. The coefficient of Young's modulus of Al is about 10 X that of AlN and perfectly accounts for the recorded experimental data.*

V. CONCLUSIONS

Design fabrication and testing of novel AlN piezoelectric NEMS resonators operating in the SHF band between 5 and 10 GHz have been demonstrated. For the first time on-chip piezoelectric sensing and actuation of nanostructures have been achieved by mechanically coupling a large number (49-99) of AlN vibrating nano-strips. AlN films have maintained high polycrystalline quality and orientation even in nanoscale devices, for which the highest $f\cdot Q$ product ($4.58\cdot10^{12}$ Hz) ever reported in NEMS resonators has been achieved. The super high frequencies of operation combined with on-chip sensing and actuation make the technology demonstrated herein amenable to the development of miniaturized components for wireless communications (WiMax, Satellite Radios and Radar), ultra sensitive chemical sensing and mechanical computing.

ACKNOWLEDGEMENT

This work was supported by NCMR/NSF grant no. IIS-07-15024 and NSF grant no. ECCS-08-22968. The authors wish to thank the staff of the Wolf Nanofabrication Facility (WNF) at The University of Pennsylvania and Chengjie Zuo and Dr. Marcelo Pisani for precious discussions.

REFERENCES

[1] M.L. Roukes, *Physics World*, 14, 25, 2001.
[2] M. Li, H. X. Tang, M.L. Roukes, *Nature Nanotechnology*, vol. 2, pp. 114-120, 2007.
[3] J. R. Vig, and F. L. Walls, *Proceedings IEEE Int. Frequency Control Symposium'00*, pp. 30-33, 2000.
[4] S. S. Verbridge et al, *Nano Letters*, vol. 7, no. 6, pp. 1728-1735, 2007.
[5] K. L. Ekinci, M.L. Roukes, *Review of Scientific Instruments*, 76, 061101, 2005.
[6] M. Hara et al, *Proceedings IEEE Ultrasonic Symposium'07*,pp. 1152-1155, 2007.
[7] P. J. Stephanou, J. P. Black, A. L. Benjamin, *Proceedings IEEE Radio Frequency Integrated Circuits Symposium'08*, pp. 171-174, 2008.
[8] G. Piazza, P.J. Stephanou, A.P. Pisano, *Journal of MicroElectroMechanical Systems,* vol. 15, no.6, pp. 1406-1418, December 2006.
[9] D. L. DeVoe, *Sensors and Actuators A,* 88, pp. 263-272, 2001.
[10] D. Weinstein, S. A. Bhave, *Proceedings IEEE International Electron Devices Meeting'07*, pp. 415-418, 2007.
[11] M. H. Cho et al, *Proceedings IEEE MTT-S Microwave Symposium'04*, pp. 1237-1240, 2004.
[12] P. J. Stephanou, A. P. Pisano, *Proceedings IEEE Ultrasonics Symposium'06*, pp. 2401-2404, 2006.
[13] R. H. Olsson III et al, *Proceedings IEEE Int. Frequency Control Symposium'08*, pp. 634-639, 2008.
[14] M. Rinaldi, C. Zuniga et al, *Proceedings IEEE Int. Frequency Control Symposium'08*, pp. 443-448, 2008.